ENTRANCE FLOW SIMULATION USING ELONGATIONAL PROPOERTIES OF PLASTICS

Mahesh Gupta
Mechanical Engineering-Engineering Mechanics Department
Michigan Technological University
Houghton, MI 49931

Abstract

A finite element simulation of the flow in a channel with an abrupt contraction is presented. Effects of shear and elongational viscosities of a polymer on the entrance flow is analyzed. The shear and elongational viscosities are represented by the truncated power-law model. The power-law index for the elongational viscosity is independent of the value of the power-law index for the shear viscosity. It is confirmed that Trouton ratio is important in determining the recirculating vortex and the extra pressure loss in entrance flow.

Introduction

In contrast to low molecular weight fluids, which can be characterized by the Newtonian constitutive equation, polymeric fluids exhibit complex rheological behavior such as strain-rate dependent shear viscosity, high resistance to elongational deformation, normal stresses in shear flow and memory of its previous configurations during a deformation [1]. Depending upon the type of flow, to model the rheology of polymers, different constitutive approaches have been used in the literature. For instance in many applications involving shear-dominated flows, such as injection molding, a generalized Newtonian constitutive equation with shear-thinning viscosity has been successfully used [2, 3]. However, in applications involving an elongational flow, such as extrusion dies, predictions from a generalized Newtonian formulation can be quite different from the real polymeric flow. Therefore, use of a constitutive equation which can predict shear as well as elongational viscosity is required for an accurate simulation of such flows. To alleviate the limitations of generalized Newtonian models, many different viscoelastic constitutive equations have been proposed in the literature [4]. Even though, many of the viscoelastic constitutive equations can qualitatively predict the phenomena such as die swell and recirculation during a creeping flow in a channel with abrupt contraction, the predictions from these equations are not always in good quantitative agreement with the corresponding experimental data [5-11]. Finding the values of various parameters such as relaxation time and viscosity for various modes in a viscoelastic constitutive equation is also difficult. Moreover, most of the numerical schemes for simulating viscoelastic flows fail to converge at high strain rates. Because of these difficulties, viscoelastic flow simulation of polymeric flow is rarely employed to resolve industrial problems.

In the present work, a software for simulation of axisymmetric polymeric flows has been developed. Besides shear viscosity, to simulate a polymeric flow this software requires a knowledge of strain-rate dependence of the elongational viscosity of the polymer. In applications involving significant elongational flow, this software can accurately predict the velocity and pressure field in the flow. This paper uses the newly developed software to analyze the effect of elongational viscosity on the recirculating vortices and pressure drop in an axisymmetric entrance flow.

Shear and Elongational Viscosities

For an axisymmetric flow, shear and elongational viscosities are, respectively defined as follows:

$$\tau_{rz} = \eta_s \dot{\gamma} \tag{1}$$

$$\tau_{zz} - \tau_{rr} = \eta_e \dot{\varepsilon} \tag{2}$$

where τ_{--} denotes various components of the stress tensor, η_s and η_e are respectively, the shear and elongational viscosities, with $\dot{\gamma}$ and $\dot{\varepsilon}$ being the corresponding strain rates. The shear and elongational viscosities of a Newtonian fluid are constant. For an axisymmetric flow of a Newtonian fluid, the Trouton ratio ($Tr \equiv \eta_e / \eta_s$) is 3. For polymers, shear and elongational viscosities depend upon strain rate. At low values of strain rate, the shear and elongational viscosities of a polymer are typically constant. For axisymmetric flow, Trouton ratio for the zero-strain-rate shear and elongational viscosities of a polymer is generally 3. As the strain rate is increased beyond the Newtonian limit, shear viscosity of a polymer decreases with increasing strain rate. For many polymers, a similar trend is observed for elongational viscosity [12 - 14]. However, for some polymers as the strain rate is increased beyond the Newtonian range, elongational viscosity increases, which is followed by a descent as the strain rate is further increased [15].

For generalized Newtonian fluids, shear viscosity is represented as a function of the second invariant of the strain rate tensor,

$$\eta_s = \eta_s(e_{II})$$

where $e_{II} = \sqrt{2(\tilde{e}:\tilde{e})}$, $\tilde{e} = (\nabla\hat{v} + \nabla\hat{v}^T)/2$ is the strain

rate tensor and $\hat{v}$ is the velocity vector. In the present work, elongational viscosity has also been represented as a function of e_{II} as defined above. It should be noted that for a simple shear flow $e_{II} = \dot{\gamma}$, whereas for an axisymmetric elongational flow $e_{II} = \sqrt{3}\,\dot{\varepsilon}$. In the literature, η_e is generally specified as a function of $\dot{\varepsilon}$ and not that of e_{II}. However, if η_s and η_e, both are specified as functions of e_{II}, it can be easily shown that irrespective of the strain rate $\eta_e = 3\eta_s$ for axisymmetric flow of all generalized Newtonian fluids.

Instead of focussing on a specific polymer, the goal of this paper is to examine the effect of elongational viscosity on entrance flow. As shown in Fig. 1, the shear and elongational viscosities have been represented by the truncated power-law model,

$$\eta_s = Ae_{II}^{n-1} \text{ for } e_{II} > e_0,\ \eta_s = \eta_0 \text{ for } e_{II} \le e_0 \qquad (3)$$

and

$$\eta_e = Be_{II}^{m-1} \text{ for } e_{II} > e_0, \eta_s = 3\eta_0 \text{ for } e_{II} \le e_0 . \qquad (4)$$

The power-law indices can be different for the shear and elongational viscosities. Elongational viscosity data for many polymers [12 - 14] can be accurately represented by a truncated power-law model. However, the initial increase in elongational viscosity beyond the Newtonian region, which is exhibited by some polymers [15], cannot be analyzed by the truncated power-law model. Even though a truncated power-law model has been used for this paper, our software can be used with any other equation specifying the strain-rate dependence of shear and elongational viscosities. For *m* = *n*, the model given by Eqns. 3 and 4 is identical to a purely viscous generalized Newtonian formulation for a truncated power-law model with power-law index of *n*.

Entrance Flow

The flow near an abrupt contraction in a channel (entrance flow) is highly extension dominated. Therefore, entrance flow is a good benchmark test for analyzing the effect of elongational viscosity on polymeric flows. Besides being a good test case, entrance flow is often encountered in polymer processing applications such as extrusion dies and runner system of injection molding. Axisymmetric entrance flow of polymers as well as that of Newtonian fluids has been investigated extensively in the literature. For Newtonian fluids it has been established experimentally and by numerical simulation that the main cause for a recirculating vortex near the abrupt contraction is the fluid inertia. In contrast, for creeping flow of polymers, it has been experimentally demonstrated by many researchers that a recirculating vortex is found near the abrupt contraction, which can grow significantly with the flow rate in the channel [16-18]. Furthermore, at certain flow rates, experiments have shown the formation of a second vortex, called lip vortex, near the entrant corner.

Since the flow near an abrupt contraction is highly extension dominated, besides the pressure drop for a fully developed flow in the upstream and downstream channels, an additional pressure loss is encountered in the entrance flow. Due to high elongational viscosity of polymers, this extra pressure loss, called entrance loss, can be particularly large for polymers. By separately calculating the pressure drop due to shear and elongational flow near an abrupt contraction, Cogswell [19] developed analytical expressions for an approximate calculation of entrance loss in a fluid with different power-law indices for shear and elongational viscosities. Such approximate expressions for entrance loss have been further refined by other researchers [20 - 24]. In references [19 - 24], power-law models have been used for shear and elongational viscosities.

Instead of approximate calculation of entrance loss, in the present work, the effect of shear and elongational viscosities of polymeric fluids has been accurately captured in the constitutive equation used for the flow simulation. Even though the finite element software has been used to simulate a 4:1 entrance flow, the software is capable of simulating any complex axisymmetric polymeric flow.

The entrance loss is generally expressed in terms of the equivalent length of the downstream channel,

$$L_e = \frac{\Delta p - \Delta p_1 - \Delta p_2}{\partial p_2} \qquad (5)$$

where Δp is the total pressure drop in the entrance flow, Δp_1 and Δp_2 are, respectively, the pressure drop for a fully-developed flow in the portions of the channel upstream and downstream of the abrupt contraction, and ∂p_2 is the magnitude of the fully-developed axial pressure gradient in the downstream channel. Trouton ratio for the strain rate at the downstream wall has been used to characterize the flow. The finite-element simulations presented later in the paper show that the Trouton ratio plays an important role in determining the recirculating vortex and extra pressure loss in entrance flow.

Effect of Elongational Power-Law Index on Entrance Flow

With the flow rate, Newtonian limit for the shear and elongational viscosities, and power-law index for shear viscosity fixed ($\dot{\gamma}_{av} = U/R = 1\ \text{s}^{-1}$, where *R* and *U* are the radius and average velocity in the downstream channel, $e_0 = 0.001\ \text{s}^{-1}$, $n = 0.25$), Fig. 2 shows the effect of elongational power-law index (*m*) on recirculating vortex in an axisym-

metric 4:1 entrance flow. For m = 0.25, which corresponds to a purely viscous generalized Newtonian formulation for the truncated power-law model with n = 0.25, no significant recirculating vortex is formed near the abrupt contraction. As the elongational power-law index is increased to m = 0.5 a small recirculating vortex is formed near the outside corner. At m = 0.55, this corner vortex grows in size and a lip vortex is also formed near the entrant corner. A further increase in the value of m to 0.58 results in a significant growth of the lip vortex. The corner vortex also grows in size, however, the vortices remain separate with two different centers of recirculation. At m = 0.6 and beyond, the two vortices coalesce together with a single center of recirculation. At m = 0.6 the center of recirculation is close to that of the lip vortex. As the elongational power-law index is further increased the recirculating vortex grows significantly and the center of recirculation moves away from the entrant corner. For n = 0.25, e_0 = 0.001 s^{-1} and $\dot{\gamma}_{av}$ = 1 s^{-1}, the entrance flow simulation converged up to m = 0.75, which corresponds to Tr = 251 (see Table 1). Even though the numerical simulation did not diverge, it failed to converge for m > 0.75. For n = 0.25, e_0 = 0.001 s^{-1}, $\dot{\gamma}_{av}$ = 1 s^{-1} and m > 0.75, the numerical simulation failed to converge even for flow simulation in a tube without any contraction. Apparently, at large values of Trouton ratio, even a small elongational flow due to computational error in the predicted velocity field for a pure shear flow gives a large elongational stresses. As the elongational stresses due to the error in the predicted velocity field start to dominate the shear stresses, even though the flow simulation in a tube (with or without a contraction) does not diverge, it fails to converge to a specific value.

For various values of elongational power-law index, Fig. 3 shows the velocity along the axis of symmetry. For m = 0.25, which corresponds to the truncated power-law model for a purely viscous generalized Newtonian fluid, a slight overshoot (0.56%) is observed in the center-line velocity. This kink in the center-line velocity is maintained as the elongational power-law index is increased, however the kink occurs at a lower velocity and a longer distance is required to reach a fully-developed velocity profile.

Normalized pressure variation along the center line for different values of m is shown in Fig. 4. The pressure has been normalized with respect to the shear stress at the wall in the downstream channel. The corresponding entrance loss is given in Fig. 5. In Fig. 4, the steep drop in pressure near the abrupt contraction, which corresponds to the entrance loss in Fig. 5, increases significantly with the elongational power-law index. At m = 0.25, the predicted entrance loss in terms of the equivalent length of the downstream channel L_e is 1.42, which agrees well with the value reported in the literature [25-28] for a purely viscous generalized Newtonian formulation for power-law model with power-law index n = 0.25. The entrance loss increases rapidly with m to a value of L_e = 29.7 for m = 0.75.

Conclusions

A finite element software for simulating axisymmetric flow of polymers has been developed. The shear and elongational viscosities of a polymer have been represented by the truncated power-law model with different power-law indices for the two viscosities. For constant values of shear viscosity parameters, the effect of power-law index for elongational viscosity on recirculating vortex and extra pressure loss in a 4:1 entrance flow has been analyzed. The recirculating vortex and extra pressure loss in an entrance flow are found to increase significantly with Trouton ratio.

References

1. R. B. Bird, R. C. Armstrong and O. Hassager, *Dynamics of Polymeric Liquids*, Vol. 1 and 2, John Wiley, New York (1987).
2. C. A. Hieber and S. F. Shen, *J. Non-Newtonian Fluid Mech.*, **7**, 1 (1980).
3. H. H. Chiang, C. A. Hieber and K. K. Wang, *Polym. Eng. Sci.*, **31**, 116 (1991).
4. R. G. Larson, *Constitutive Equations for Polymeric Melts and Solutions*, Butterworths, Boston (1988).
5. R. Keunings, Chapter 9 in *Fundamentals of Computer Modelling for Polymer Processing*, C. L. Tucker (ed.), Hanser, Munich (1989).
6. B. Debbaut, J. M. Marchal and M. J. Crochet, *J. Non-Newtonian Fluid Mech.*, **29**, 119 (1988).
7. D. Rajagopalan, R. C. Armstrong and R. A. Brown, *J. Non-Newtonian Fluid Mech.*, **36**, 159 (1990).
8. B. Purnode, M. J. Crochet, *J. Non-Newtonian Fluid Mech.*, **65**, 269 (1996).
9. M. Gupta, C. A. Hieber and K. K. Wang, *Int. J. Numer. Meth. Fluids*, **24**, 493 (1997).
10. C. Beraudo, A. Fortin, T. Coupez, Y. Demay, B. Vergnes, J. F. Aggasant, *J. Non-Newtonian Fluid Mech.*, **75**, 1 (1998).
11. S. C. Xue, N. Phan-Thein, R. I. Tanner, *J. Non-Newtonian Fluid Mech.*, **74**, 195 (1998).
12. H. M. Luan, in *Rheology*, Vol. 2, G. Astarita, G. Marrucci and L. Nicolais (eds.), Plenum, New York 419-424 (1980).
13. H. Munstedt and H. M. Luan, *Rheol. Acta*, **20**, 211 (1981).
14. J. A. van Aken and H. Janeschitz-Kriegl, *Rheol. Acta*, **19**, 744 (1980); **21**, 388 (1982).
15. H. M. Luan and H. Schuch, *J. Rheol.*, **33**, 119 (1989).
16. D. V. Boger, *Annu. Rev. Fluid Mech.*, **19**, 157 (1987).
17. J. A. White, A. D. Gotsis and D. G. Baird, *J. Non-Newtonian Fluid Mech.*, **24**, 121 (1987).
18. R. E. Evan and K. Walters, *J. Non-Newtonian Fluid Mech.*, **32**, 95 (1989).

19. F. N. Cogswell, *Polym. Eng. Sci.*, **12**, 64 (1972).
20. A.G. Gibson and G. A. Williamson, *Polym. Eng. Sci.*, **25**, 968 and 980 (1985).
21. T. H. Kwon, S. F. Shen and K. K. Wang, *Polym. Eng. Sci.*, **26**, 214 (1986).
22. D. M. Binding, *J. of Non-Newtonian Fluid Mech.*, **27**, 173 (1988).
23. M. Gupta, C. A. Hieber and K. K. Wang, *SPE ANTEC Tech. Papers*, **41**, 774 (1995).
24. M. E. Mackay, G. Astarita, *J. Non-Newtonian Fluid Mech.*, **70**, 219 (1997).
25. D. V. Boger, R. Gupta and R. I. Tanner, *J. Non-Newt. Fluid Mech.*, **4**, 239 (1978).
26. M. E. Kim-E, R. A. Brown and R. C. Armstrong, *J. Non-Newt. Fluid Mech.*, **13**, 341 (1983).
27. C. A. Hieber, *Rheol. Acta*, **26**, 92 (1987).
28. M. Gupta, C. A. Hieber and K. K. Wang, *Polym. Eng. Sci.*, **34**, 209 (1994).

Key words: Elongational viscosity, Extensional viscosity, Extrusion, Entrance Flow.

Table 1

Trouton ratio at the downstream channel wall in a 4:1 contraction for $n = 0.25$, $e_0 = 0.001\ s^{-1}$, $\dot{\gamma}_{av} = 1\ s^{-1}$.

m	0.25	0.35	0.45	0.55	0.65	0.75
Tr	3.0	7.3	17.6	42.7	103.6	251.0

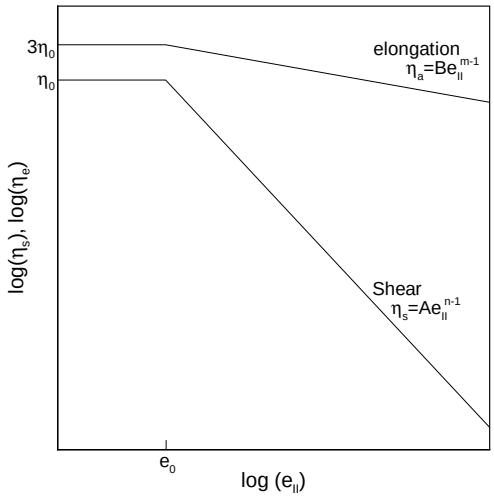

Fig. 1. Truncated power-law model for shear and elongational viscosities.

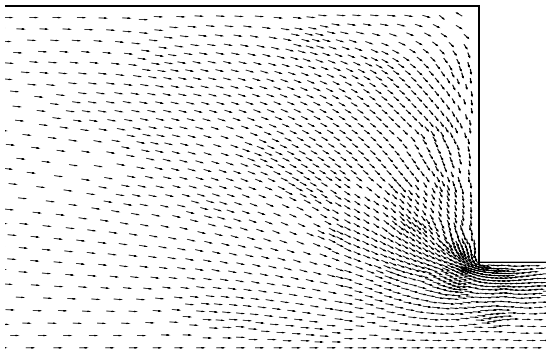

(a)

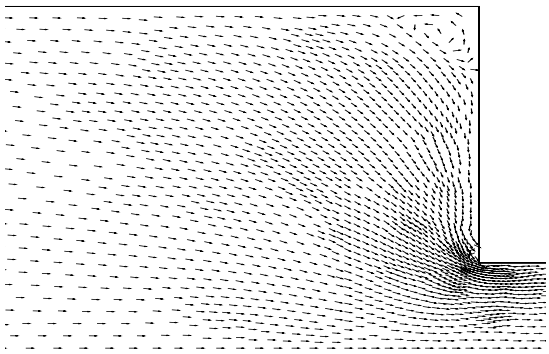

(b)

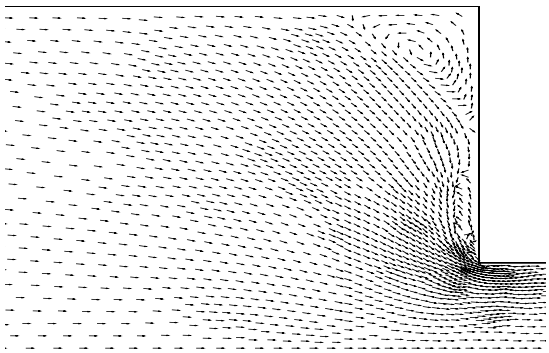

(c)

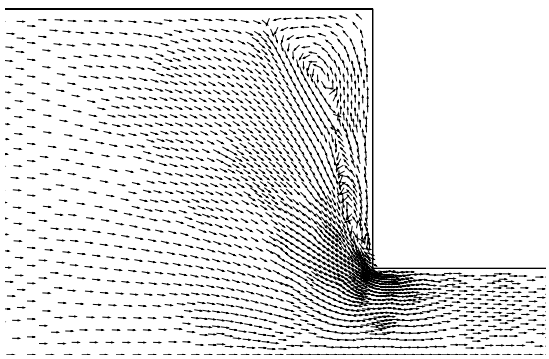

(d)

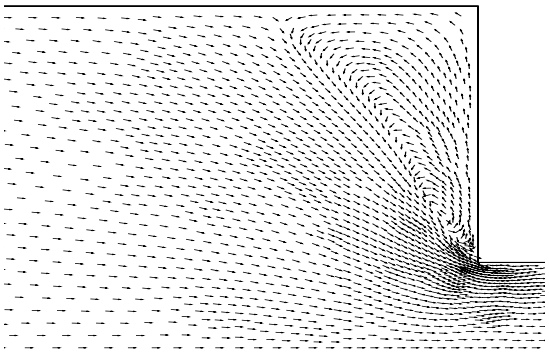

(e)

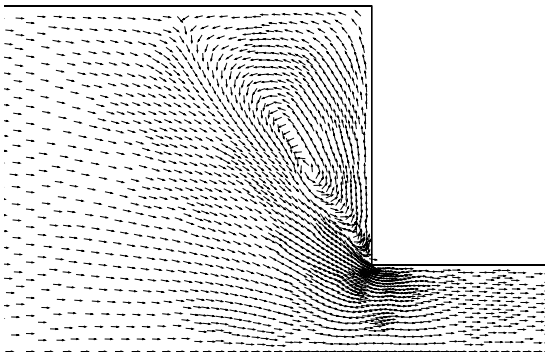

(f)

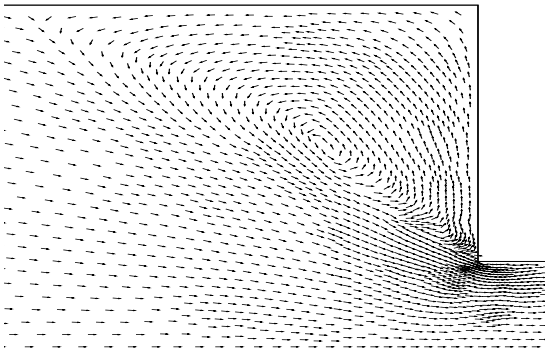

(g)

Fig. 2. Recirculation in 4:1 abrupt contraction for n = 0.25, e_0 = 0.001 s^{-1} and $\dot{\gamma}_{av}$ = 1 s^{-1}. The elongational power-law index, m, is (a) 0.25, (b) 0.5, (c) 0.55, (d) 0.58, (e) 0.6, (f) 0.65, (g) 0.75.

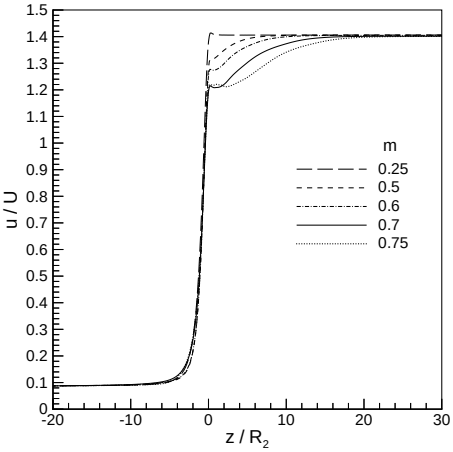

Fig. 3. Velocity along the axis of symmetry for n = 0.25, e_0 = 0.001 s^{-1}, $\dot{\gamma}_{av}$ = 1 s^{-1} and various values of the elongational power-law index.

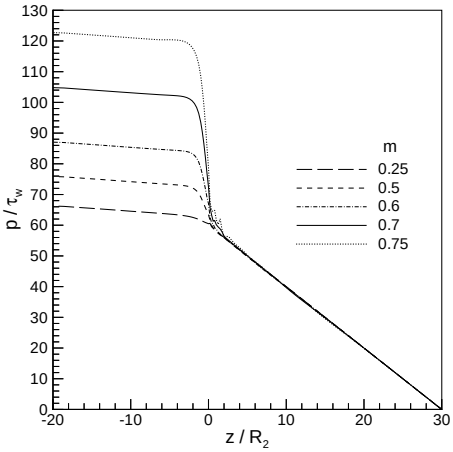

Fig. 4. Pressure along the axis of symmetry for n = 0.25, e_0 = 0.001 s^{-1}, $\dot{\gamma}_{av}$ = 1 s^{-1} and various values of the elongational power-law index.

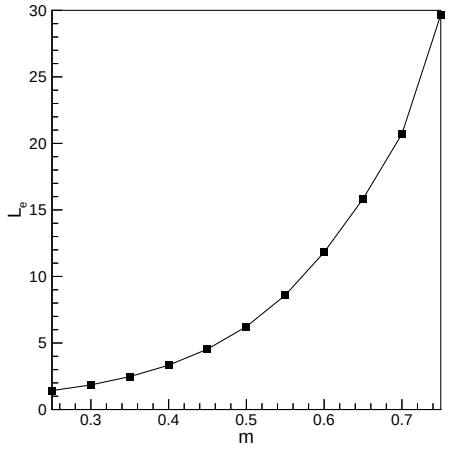

Fig. 5. Entrance loss vs. m for n = 0.25, e_0 = 0.001 s^{-1} and $\dot{\gamma}_{av}$ = 1 s^{-1}.